HHS Public Access

Author manuscript

Dev Neurobiol. Author manuscript; available in PMC 2017 May 01.

Published in final edited form as:

Dev Neurobiol. 2016 May ; 76(5): 533–550. doi:10.1002/dneu.22330.

Aryl Hydrocarbon Receptor (AhR) Deletion in Cerebellar Granule Neuron Precursors Impairs Neurogenesis

Daniel P. Dever[1], **Zachariah O. Adham**[1], **Bryan Thompson**[1], **Matthieu Genestine**[2], **Jonathan Cherry**[3], **John A. Olschowka**[4], **Emanuel DiCicco-Bloom**[2], and **Lisa A. Opanashuk**[1]

[1]Department of Environmental Medicine, University of Rochester School of Medicine and Dentistry, Rochester, New York, 14642

[2]Department of Neuroscience and Cell Biology, Robert Wood Johnson Medical School, Rutgers, The State University of New Jersey, Piscataway, New Jersey 08854

[3]Department of Pathology and Laboratory Medicine, University of Rochester School of Medicine and Dentistry, Rochester, New York, 14642

[4]Department of Neurobiology and Anatomy, University of Rochester School of Medicine and Dentistry, Rochester, NY 14642

Abstract

The aryl hydrocarbon receptor (AhR) is a ligand-activated member of the basic-helix-loop-helix (bHLH)/PER-ARNT-SIM(PAS) transcription factor superfamily that also mediates the toxicity of 2,3,7,8-tetrachlorodibenzo-*p*-dioxin (TCDD). Increasing evidence suggests that AhR influences the development of many tissues, including the central nervous system. Our previous studies suggest that sustained AhR activation by TCDD and/or AhR deletion disrupts cerebellar granule neuron precursor (GNP) development. In the current study, to determine whether endogenous AhR controls GNP development in a cell autonomous manner, we created a GNP-specific AhR deletion mouse, $AhR^{fx/fx}$/$Math1^{CRE/+}$ (AhR CKO). Selective AhR deletion in GNPs produced abnormalities in proliferation and differentiation. Specifically, fewer GNPs were engaged in S-phase, as demonstrated by ~25% reductions in thymidine (*in vitro*) and BrdU (*in vivo*) incorporation. Furthermore, total granule neuron numbers in the IGL at PND21 and PND60 were diminished in AhR CKO mice compared to controls. On the other hand, differentiation was enhanced, including ~40% increase in neurite outgrowth and 50% increase in GABARα6 receptor expression in deletion mutants. Our results suggest that AhR activity plays a role in regulating granule neuron number and differentiation, possibly by coordinating this GNP developmental transition. These studies provide novel insights for understanding the normal roles of AhR signaling during cerebellar granule cell neurogenesis, and may have important implications for the effects of environmental factors in cerebellar dysgenesis.

Corresponding author: Daniel P. Dever, PhD, Department of Pediatrics, Lorry Lokey Stem Cell Research Building, 269 Campus Drive, Room G3045, Stanford University, Stanford CA, 94305, ddever1@stanford.edu.

Conflict of interests: No conflicts of interests exist.

Keywords

Aryl hydrocarbon receptor; cerebellar granule cells; cerebellum development; neurogenesis

INTRODUCTION

The final number of granule neurons in the cerebellum is determined by the balance between granule neuron precursor cell (GNP) proliferation, differentiation, and cell death, processes that are coordinated by an assortment of intrinsic and extrinsic factors (Hatten and Heintz, 1995; Hatten *et al.*, 1997; Wang and Zoghbi, 2001; Roussel and Hatten, 2001; Nicot and DiCicco-Bloom, 2001). GNPs are born in the rhombic lip between embryonic days (E) E12-E15, where they undergo clonal expansion and migrate rostrally to form the external granule layer (EGL) during rodent cerebellar development (Hatten *et al.*, 1997 and Wang and Zoghbi, 2001). GNPs proliferate extensively during postnatal days (PND) 5-10 in the developing mouse cerebellum. Several mitogens have been identified, which include sonic hedgehog (Shh), basic fibroblast growth factor (bFGF) and insulin-like growth factor (IGF) (Kenney *et al.*, 2003; Cheng *et al.*, 2001; Ye *et al.*, 1996). Shh is secreted by Purkinje cells and has been reported to be one of the most efficacious mitogens in GNPs *in vivo* and *in vitro* (Kenny and Rowitch, 2000; Wechsler-Reya and Scott, 1999). These mitogenic signaling pathways induce expression of pro-proliferative genes such as N-myc, Cyclin D, Cyclin B, Cyclin E and Hes1 (Corrales *et al.*, 2006; Kenney *et al.*, 2003; Duman-Scheel *et al.*, 2002; Solecki *et al.*, 2001). Following the peak in proliferation, GNPs exit the cell cycle, and then migrate inward toward the IGL between PND4-15 (Hatten *et al.*, 1997). Cell cycle exit begins in the inner EGL, where cell cycle inhibitors, such as $p27^{KIP1}$, act to promote cell cycle exit (Miyazawa *et al.*, 2000). Later stages of granule cell development are also characterized by well-defined patterns of gene expression that coordinate migration and terminal differentiation, such as astrotactin and $GABAR_{A\alpha 6}$ (Zheng *et al.*, 1996 and Zheng *et al.*, 1993).

Several bHLH/PAS transcription factor proteins are known to regulate granule neuron development (Crews, 1998 and Crew and Fan, 1999). For example, Nmyc1 has been shown to promote GNP proliferation, while Zic1 and NeuroD1 initiate granule cell differentiation (Kenney *et al.*, 2004; Aruga *et al.*, 2002; Miyata *et al.*, 1999). Math-1, the mouse homologue of the *Drosophilia* gene Atoh-1, is expressed in GNPs on embryonic day 13 (E13) and this expression is maintained until the cells exit the cycle and begin migration to the internal granule cell layer (IGL) (Machold and Fishell, 2005). Significantly, when Math-1 is deleted, the EGL is entirely missing in the postnatal mouse (Ben-Arie *et al.*, 1996). Another bHLH/PAS transcription factor, Hes1, has been reported to maintain GNPs in their precursor state, an action that may depend on repressing expression of $p27^{KIP1}$ (Solecki *et al.*, 2001 and Murata *et al.*, 2005). Interestingly, our previous studies indicate that the aryl hydrocarbon receptor (AhR) is highly expressed and transcriptionally active during the critical period of GNP expansion and maturation (Williamson *et* al., 2005 and Hatten *et al.*, 1997). These observations led us to hypothesize that AhR plays a cell autonomous role in promoting GNP proliferation.

Although it serves as a transcription factor, the AhR is also an environmental sensor that responds to numerous exogenous ligands (endogenous ligands remain undefined), most notably the ubiquitous and persistent environmental contaminant 2,3,7,8-tetrachlorodibenzo-*p*-dioxin (TCDD; dioxin) (Denison and Nagy, 2003). Indeed, major insights into AhR's roles in brain development have been obtained by investigating the toxicity of TCDD, the most potent ligand (Birnbaum and Tuomisto, 2000). Initial studies showed that low dose perinatal dioxin exposure in rodents impaired adult learning, memory and motor function, all behaviors associated with the cerebellum (Schantz, 1996; Kakeyama and Tohyama, 2003; Thiel *et al.*, 1994). Because these studies suggested dioxin perturbed AhR functions in the cerebellum, we investigated its expression profile. GNPs expressed robust levels of transcriptionally-active AhR during their postnatal expansion with levels declining during differentiation, but continuing through adulthood (Williamson *et al.*, 2005). To begin defining the role of AhR in cerebellar biology, we investigated the impact of dioxin exposure on GNP development. Low-dose TCDD exposure during the postnatal proliferative phase resulted in premature GNP maturation and compromised cell survival, ultimately decreasing adult cerebellar cell number (Collins *et al.*, 2008). We hypothesized that GNP development was dysregulated because TCDD diverted AhR from its endogenous functions (Collins *et al.*, 2008). Collectively, these studies suggest that AhR plays a role in cerebellar granule cell development, which can be perturbed by TCDD and potentially other AhR ligands.

In addition to toxicological evidence, genetic studies also indicate that AhR contributes to development. For example, $AhR^{-/-}$ mice exhibit defects in vascular, reproductive, cardiac, and brain systems (Lahvis *et al.*, 2005; Lund *et al.*, 2003; Schmidt *et al.*, 1996; Collins *et al.*, 2008). Furthermore, in invertebrates, loss of AhR function impacts cell fate decisions, differentiation, migration, and dendrite growth during neurogenesis (Huang *et al.*, 2004; Qin and Powell-Coffman, 2004; Kim *et al.*, 2006). Therefore, we considered the possibility that AhR may perform similar functions during development of the cerebellum. Indeed, in the cerebella of adult mice with global AhR deletion, we found reduced cell numbers (Collins *et al.*, 2008). Moreover, GNPs from $AhR^{-/-}$ mice extended neurites earlier than their wild type counterparts, suggesting AhR may regulate the transition from cell proliferation to differentiation in GNPs (Collins *et al.*, 2008). While these global gene deletion studies suggest AhR has conserved function(s) during CNS development, its normal functions in GNP during neurogenesis remain to be identified.

In this study, we tested the hypothesis that the AhR has a cell-autonomous role in regulating the development of GNPs. We created a GNP-specific AhR knockout mouse ($AhR^{fx/fx}$/$Math1^{CRE/+}$) utilizing the Cre-LoxP conditional knockout strategy, which resulted in GNPs with decreased AhR expression. Our data demonstrate that the loss of AhR expression in GNPs negatively impacted granule neuron number. Furthermore, AhR CKO GNPs showed a reduction in GNP proliferation and an increase in neurite outgrowth, suggesting a putative role(s) for AhR in regulating proliferation and/or differentiation during cerebellar granule cell neurogenesis. Our findings suggest that AhR participates in the production and development of cerebellar granule neurons, possibly through controlling the transition between GNP proliferation and differentiation.

MATERIALS AND METHODS

Reagents

Phenylmethanesulfonyl (PMSF), antiprotease cocktail, Triton X-100, Hoechst 33258 and bovine serum albumin (BSA) were purchased from Sigma (St. Louis, MO). Dulbecco's modified Eagle's medium (DMEM), penicillin/streptomycin, fetal bovine serum (FBS), EDTA and L-glutamine were purchased from Gibco (Grand Island, NY). [3-(4,5-dimethylthiazol-2-yl)-5-(3-carboxymethoxyphenyl)-2-(4-sulfophenyl)-2H-tetrazolium, inner salt; MTS] was purchased from Promega (Madison, WI).

Experimental Animals

Math1$^{Cre/+}$ mice were created and generously provided by Dr. Lin Gan (University of Rochester Medical Center, Rochester, NY) (Yang *et al.*, 2010). AhR$^{fx/fx}$ and mT/mG mice were kindly provided by Dr. Paige Lawrence and Dr. Michael O'Reilly, respectively (University of Rochester Medical Center, Rochester, NY) (Walisser *et al.*, 2005 and Muzumdar *et al.*, 2007). AhR$^{fx/fx}$/Math1$^{Cre/+}$ (AhR CKO) and AhR$^{fx/fx}$/Math1$^{+/+}$ (Control) mice were generated by crossing male AhR$^{fx/fx}$/Math1$^{Cre/+}$ mice with female AhR$^{fx/fx}$/Math1$^{+/+}$ mice. mTmG$^{+/-}$/AhR$^{fx/+}$/Math1$^{Cre/+}$ and mTmG$^{+/-}$/AhR$^{fx/+}$/Math1$^{+/+}$ mice were generated by mating female mT/mG$^{+/+}$/AhR$^{+/+}$/Math1$^{+/+}$ mice with male mT/mG$^{-/-}$/AhR$^{fx/fx}$/Math1$^{Cre/+}$. The PCR primers used to identify Math1$^{Cre/+}$ alleles were Math1$^{Cre/+}$-F1 (5'-GCG CAG CGC CTT CAG CAA C-3') and Math1$^{Cre/+}$-R1 (5'-GCC CAA ATG TTG CTG GAT ATG-3'), and primers used to identify AhR excised alleles were excised-F1 (5'- GTC ACT CAG CAT TAC ACT TTC TA-3') and excised-R1 (5'- GGT ACA AGT GCA ACA TGC CTG C-3'), and primers used to identify AhR unexcised alleles were unexcised-F1 (5'-CAG TGG GAA TAA GGC AAG AGT GA-3') and unexcised-R1 (5'-GGT ACA AGT GCA ACA TGC CTG C-3'), and primers used to identify mT/mG WT-F1 (5'-CTC TGC TGC CTC CTG GCT TCT-3'), and mT/mG WT-R1 (5'-CGA GGC GGA TCA CAA GCA ATA-3'), and mT/mG MT-R1 (5'-TCA ATG GGC GGG GGT CGT T-3'). Mice were maintained on a 12 hour light/dark cycle with food and water provided ad libitum and kept in accordance with the guidelines set by the University of Rochester University Committee on Animal Resources and the American Association for Laboratory Animal Science. The mouse strains were maintained in the C57BL/6J mixed background.

DNA Content Analysis

DNA content was quantified as a surrogate measure of cell number with the fluorescent DNA-binding dye bisbenzimidazole (Hoechst 33258) following a protocol as previously described (Collins *et al.*, 2008). Tissues were homogenized in 50mM sodium phosphate, 2M NaCl, 2 mM ethylenediaminetetraacetic acid (pH 7.4). Hoechst was added to samples at a final concentration of 1 μg/ml and samples were read in a spectrofluorometer using an excitation wavelength of 356 nm and an emission wavelength of 458 nm. The amount of DNA in each sample was calculated by linear regression with purified calf thymus DNA used as a standard (Labarca and Paigen, 1980).

Immunoblot Analysis

Protein levels were analyzed by immunoblot analysis as previously described (Williamson *et al.*, 2005 and Collins *et al.*, 2008). Cerebella were harvested for protein analysis in ice-cold PBS supplemented with 0.1 % Triton X-100, 1.0 % phenylmethanesulfonyl (PMSF), 1.0 % EDTA and 1.0 % antiprotease cocktail. Protein concentrations were determined by using the microBCA protein assay (Pierce, Rockford, IL). Protein (10μg) was fractionated on 10% polyacrylamide gels and transferred to polyvinylidene difluoride membranes (BioRad, Hercules, CA). Membranes were subsequently blocked with 5% powdered milk containing 0.2% Tween-20 and probed for β-actin (1:5000; Sigma, St. Louis, MO), $GABAR_A\alpha6$ (1:1000; Chemicon, Temecula, CA), or Calbindin (1:1000; Sigma) overnight at 4°C. Following overnight incubation, membranes were incubated with the appropriate horseradish peroxidase-conjugated secondary antibody (Jackson Immunoresearch Laboratories, Bar Harbor, MA) for 1h at room temperature. Proteins were visualized with LumiGLO chemiluminescent substrate reagent (Kirkegaard & Perry Laboratories, Gaithersburg, MD). Semi-quantitative densitometric analysis of proteins was accomplished with ImageJ software (National Institutes of Health).

BrdU Administration

To analyze cell fate, cells in S phase on PND10 were labeled using 50 mg/kg Bromodeoxyuridine (BrdU) administered by intraperitoneal injection (i.p.). On PND21 and PND60, AhR CKO and Control mice were perfused, first with saline, then with 4% paraformaldehyde, via cardiac puncture and brains were harvested. Brains were then further fixed in 4% paraformaldehyde overnight and transferred to 30% sucrose the next day. To quantify the number of GNPs in S phase on PND10, AhR CKO and Control mice were ip injected with 50 mg/kg BrdU and were perfused 2 hours later. Tissue was processed for the immunohistochemical detection of BrdU incorporation as described below.

Immunohistochemistry

Immunohistochemistry was carried out as previously described (Williamson *et al.*, 2005 and Collins *et al.*, 2008). Cerebella were sectioned parasagittally on a freezing sliding microtome at 30 μm, collected in cryoprotectant, and stored at −20°C until tissue staining. Free-floating sections were rinsed in PBS containing 0.3% triton (PBST). For BrdU staining, sections were incubated with 2M HCL for 60 minutes, rinsed, incubated in 3% H2O2 for 30 minutes, and then rinsed again. Tissues were blocked with 10% normal goat serum, then incubated with $GABAR_A\alpha6$ (1:750; Chemicon), Calbindin (1:750; Sigma), BrdU (1:800; Sigma), phosphorylated histone 3 (pH3; 1:400; Millipore, Billerica, MA), glial fibrillary acidic protein (GFAP; 1:4000; Millipore), or Myelin Basic Protein (MBP; 1:100; Chemicon). Following overnight incubation with respective primary antibodies, tissue was rinsed with PBST and incubated with the appropriate Alexa Fluor 488-conjugated or 594-conjugated secondary antibodies (1:750; Molecular Probes, Eugene, OR) for 90 minutes at room temperature. Cell nuclei were identified with 1 μg/ml 4', 6-diamidino-2-phenlindole (DAPI) staining. Staining for AhR CKO and control cerebellar tissues was carried out on the same day. Fluorescence was visualized with an Olympus FV1000 laser scanning confocal microscope (University of Rochester). Z-stack images were taken and collapsed with the

Olympus FV1000 software program. Positive staining was not observed when tissue was incubated with secondary antibody alone.

In Vivo IGL Cell Counts

Cells positive for BrdU were counted in 4-6 parasagittal sections in folium III using a 1:12 sectioning series from at least 5 animals per genotype. Cells were counted blind using the automated cell counting system explained below in the same region of the central vermis and were not counted in the vermis-hemisphere boundary, or the hemisphere. Automated cell counts were accomplished using the ImageJ plugin, Image-based Tool for Counting Nuclei (ITCN) (Loukas *et al.*, 2003). The inputs are: 1) an estimation of cell diameter, 2) an estimation of the minimum distance between cells, and 3) determining threshold for positive staining. Images were opened in ImageJ and converted to 8-bit. ITCN plugin was launched and cell width, distance, and staining threshold was determined for all images in the set (at least 4-6 sections per animal). Regions of interest were selected, IGL for PND21 and PND60 cerebellar slices, and automated counts were obtained. Then, the areas of the regions selected were calculated and cells/mm^2 values were obtained. 4-6 values of cells/mm^2 were averaged together to obtain values for each animal and 5 animals were used per genotype.

In Vivo EGL Cell Counts

Cerebella from PND10 AhR CKO and control mice were serially sectioned parasagittally as described above. GNPs were counted blind in the same region of the central vermis for all mice and were not counted in the vermis-hemisphere boundary, or the hemispheres. For BrdU studies, a 100μm wide frame was placed in the central region of folium III and positive cells in the EGL were counted. BrdU and pH3 positive GNPs were counted in 4-6 sections in folium III using a 1:12 sectioning series from at least 5 animals per genotype. The number of BrdU and DAPI positive cells were counted with ImageJ (described above) and BrdU labeling index was defined as the number of BrdU-positive cells/total DAPI cells ×100% for each genotype. Approximately 1000 EGL cells were counted in total from the 4-6 sections that were assessed in each animal.

TUNEL Assay

The In Situ Cell Death Detection (Roche) kit was used to detect apoptotic cells *in vivo*. 30 μm PND10 cerebellar parasagittal sections were rinsed with PBS three times for 10 minutes and permeabilized with PBST for 10 minutes on ice. Sections were mounted on slides and allowed to dry. 50μl TUNEL reaction mixture was added on to the sections and incubated at 37°C for 1 hour. TUNEL positive cells were counted in 4-6 sections of folium III from 3 animals per genotype. Sections treated with 5units/ml DNase I for 30 minutes to induce double strand breaks served as positive controls for the TUNEL assay. Cerebellar tissue incubated without the terminal transferase enzyme was used as the negative controls.

Reaggregate GNP Cultures

Primary cerebellar granule cell neuroblasts were isolated and cultured as previously described (Williamson *et al.*, 2005 and Collins *et al.*, 2008). Cerebella from postnatal day 10 AhR CKO or control mice were dissected and after removing the meninges, tissues were cut

into pieces. After adding DNase, tissues were mechanically dissociated using glass pipettes. Dissociated cells were passed through a 30μm filter and centrifuged through a 35%: 60% Percoll gradient. Cells were rinsed and pre-plated for 60 minutes on poly-d-lysine coated T-25 flasks (VWR, Radnor, PA) and resuspended in DMEM containing 10% horse serum, 5% fetal bovine serum, 9 mg/ml glucose, 292 mg/ml glutamine, and 0.1% penicillin. Cells were counted and plated in a 96-well plate at a density of 3×10^5 cells/well and maintained overnight in a humidified atmosphere of 5% CO_2 at 37°C to promote reaggregate formation.

Low Density GNP Cultures

Cerebellar granular neuron cultures from B6/C57 mice at postnatal days 5 to 8 were adapted from previously describe protocols (Rossman., *et al* 2004). Briefly, 3 to 6 cerebella were cleaned, dissociated by 3 min treatment with trypsin-DNase (1% trypsin, 0.1% DNase, Worthington, Lakewood, NJ) and triturated in DNase solution (0.05% in DMEM). Then the cells were filtered (30-um nylon mesh; Tekton, Tarrytown, NY), before being centrifuged on a Percoll (Sigma, St. Louis, MO) step gradient 35:60%. Cells at the interface were washed and pre-plated for one hour onto a poly-D-lysine (0.1 mg/ml) coated dish in culture media. The culture media was composed of glutamax, 50 U/ml penicillin and 50ug/ml streptomycin, 0.9% sucrose, 10% horse serum and 5% fetal bovine serum in BME. Then loosely adherent cells were detached and 2×10^6 cells were plated on a 35mm dishes coated with a poly-D-lysine, 2 dishes each group. At 24h after platting, considered as 1 day *in vitro* (1 DIV), cells were infected with an empty or AhR-shRNA lentiviral vector at 10 Multiplicity of infection (MOI). The vector contained a Puromycin resistance gene (see below lentivirus production method). At 48 hours after infection (3DIV), successfully infected cells were selected for 24 hours by using 1 μg/ml of Puromycin. Finally the cultures were fixed with 4% paraformaldehyde for 20 min, washed with PBS and coverslipped before analysis of neurite length per CGN (see below quantification method).

[^{3}H]Thymidine Incorporation

GNPs were aggregated for 48 hours in a 96-well plate at a concentration of 3×10^5 cells/well in media with 10% serum, or serum-free media containing 3μg/ml sonic hedgehog (a generous gift from Dr. Anna M. Kenney, Emory University). During the last 24 hours, GNPs were labeled with 1μCi of methyl-^{3}H- thymidine (Perkin Elmer)/ml and harvested onto filter paper using a Skatron cell harvester. The amount of incorporated radioactivity was quantified by liquid scintillation counting (Dever and Opanashuk, 2012).

GNP Differentiation

GNPs from AhR CKO or control cerebella were aggregated overnight as described above. Following a 24hr aggregation period, the cells from two (2) 96-wells (6×10^5 cells) were seeded into one (1) 24-well (BD Falcon) containing german-glass micro glass (Electron Microscopy Sciences, Hatfield, PA) coverslips coated with 0.1 mg/ml poly-L-lysine on the bottom of each well. Cells were incubated with serum-free DMEM medium supplemented with B27 and N2 to promote neurite outgrowth for 48 hours. GNPs were fixed and processed for immunocytochemistry as described below.

Immunocytochemistry

Immunocytochemistry was carried out as previously described (Williamson *et al.*, 2005; Collins *et al.*, 2008; Dever and Opanashuk, 2012). After 48h in differentiation culture conditions, cells were rinsed with DPBS and then fixed with 4% paraformaldehyde at room temperature for 30 min. After fixation, cells were blocked in PBS containing 10% normal goat serum and 0.3% Triton-X-100 at room temperature for 30 min. Fixed cells were then incubated with an AhR antibody (1:800; Enzo) or βIII-tubulin antibody (1:100; Chemicon) overnight at 4°C. Following overnight incubation, cells were washed and incubated with the appropriate Alexa Fluor-conjugated secondary antibody (Molecular Probes) for 90 min at room temperature. Nuclei were stained with DAPI (1:5000; Molecular Probes) for fixed cell imaging. Fluorescence was visualized with an Olympus FV1000 laser scanning confocal microscope. Z-stack images were taken with the Olympus FV1000 software program. Positive staining was not observed when cells were incubated with secondary antibody alone.

Lentivirus production

Human embryonic kidney 293FT cells (Invitrogen) were grown to 60–80% confluency in Dulbecco's modified Eagle's media (GIBCO) supplemented with 10% fetal bovine serum in T-175 flasks. The VSVG pseudotyped HIV vector was generated by co-transfecting with 7.3μg of envelope plasmid (pMD2G), 18.2μg of packaging plasmid (psPAX2), and 18.2μg transfer vector (shRNA mAhR or Empty), using lipofectamine LTX (Invitrogen). Media was changed 6 hours post-transfection. Viral supernatants were harvested at 48, 72 and 96 hours post-transfection. Viral supernatants were spun down twice for 5 minutes at 2,000$^{\times}$g and filtered through a .45μm low protein-binding filter. Viruses were concentrated 1000 fold using Lenti-X concentrator (Clontech). The concentrated viruses were stored at −80° C until use.

Quantitative real time polymerase chain reaction (Q-PCR)

RNA was harvested from PND 6, 8, 15 AhR CKO or control GNPs using the RNeasy Mini Kit (Qiagen). 1μg of RNA was reverse transcribed into cDNA using the Super Script III First-Strand cDNA Synthesis Kit (Invitrogen). cDNA was prepared using 1 μg of RNA, oligo (dT) and random hexamer primers, and SuperScript III (Invitrogen). qRT-PCR for 18S used Taqman probe/primer sets and were designed as follows: from 5' to 3' 18S, forward primer (F), cct gga tac cgc agc tag gaa, reverse primer (R), act aag aac ggc cat gca cca, and probe (P), cgg cgg cgt tat tcc cat gac c. Primer/probe sets were constructed with FAM as the fluorescent marker and Blackhole I quencher (Biosearch Technologies, Navato, CA). For cdkn18, cntn2, atoh1, hesx1, p57, cyclin d5, and neuroD predesigned primer/probe sets were purchased (Applied Biosystems, Carlsbad, CA). PCR reactions were performed using iQsupermix (Bio-Rad, Hercules, CA) and 1 μl of cDNA. PCR conditions were as follows: denaturation at 95°C for 3 min, followed by 40 cycles of amplification by denaturing at 95°C for 30 second, annealing at 60°C for 30 seconds, and extension at 72°C for 30 seconds. To determine relative differences in mRNA, reaction efficiency (E) was calculated from a standard curve and cycle threshold (Ct) values were transformed using the equation

expression = $(1+E)^{Ct}$. For normalization, 18S ribosomal RNA was used as the housekeeping gene.

Quantifying Neurite Outgrowth

Neurite outgrowth was assessed using the ImageJ plugin, NeuriteTracer (Pool *et al.*, 2008). βIII-tubulin (length of neurites) and DAPI (circumference of neurospheres) stained images were opened and converted to 8-bit images. NeuriteTracer automatically calculated length of neurites (μm) and neurosphere circumference (mm^2). The scale was calibrated using 100μm scale bars obtained from an Olympus FV1000 laser scanning confocal microscope. Values are reported as length of neurites per area of neurosphere ($\mu m/mm^2$). For low density GNP cultures, 4 images per petri dish of differentiated GNPs were taken using a phase contrast magnification of 40× with a Zeiss microscope Axiovert 200 M. Fields were acquired at predefined positions 1cm apart. Cell number and neurite density were analyzed with ImageJ software. Neurite densities were estimated by counting each intersection of neurites with 4 verticals and 4 horizontal virtual lines.

MTS Assay

Cell Titer 96 AQueous One Solution Cell Viability Assay (Promega) was used to determine viability of wildtype and AhR deficient GNPs *in vitro*. Following a 24 hour aggregation in a 96-well plate, 20 μl MTS reagent was added to 100 μl media containing GNP suspended aggregates for 4 hours at 37°C. Values were obtained using a spectrophotometer by reading absorbances at 490 nm. Viability values were quantified as a percent of control.

Statistical Analysis

Data are expressed as means +/− standard error of the mean (SEM). Sample sizes are indicated in the figure legends. Most of the statistical analyses were performed by Student's *t*-tests, but multiple comparisons were analyzed by a two-way ANOVA. P values of <0.05 were considered statistically significant.

RESULTS

Cre recombinase is robustly expressed in cerebellar GNPs via the Math1 promoter, which results in excision of AhR alleles and a reduction in AhR protein levels

The purpose of these studies was to determine whether AhR has an intrinsic role in regulating the development of cerebellar granule neurons. We developed a mouse model, using the Cre/LoxP strategy, to specifically knockout AhR within the granule neuron precursor population (GNPs), by using GNP-specific Math1 to drive Cre mediated excision. We used the double-fluorescent mT/mG reporter mouse to verify that Math1-cre was expressed in the GNP target population (Muzumdar *et al.*, 2007). We confirmed that GNPs, which reside in the EGL, exclusively expressed mG, indicating the presence of Cre recombinase activity (Fig. 1A, bottom left panel). Green signal was not detected in the molecular or Purkinje cell layers of the cerebellum (data not shown). Additionally, we isolated GNPs from mTmG/$AhR^{fx/+}$/$Math1^{Cre/+}$ mice and further confirmed they robustly express green signal indicating Cre activity (Fig. 1B, bottom left panel), which was absent from the control (Fig. 1B, bottom right panel). These studies confirm that $Math1^{Cre/+}$ mice

express Cre in GNPs *in vivo* and when mated with $AhR^{fx/fx}$ mice, should give rise to GNPs that target AhR alleles for Cre-mediated excision.

To determine whether Cre-mediated recombination of AhR alleles occurs in GNPs, genomic DNA was isolated from AhR CKO and control GNPs. Excised alleles, characterized by a 40bp shift from 140bp to 180bp as previously reported (Walisser et al., 2005), were only detected in AhR CKO GNPs, indicating that Cre targets AhR floxed alleles (Fig. 2A). In order to determine if excision of AhR alleles resulted in a reduction of AhR protein expression, cultured PND10 GNPs from AhR CKO and control mice were probed for AhR expression, via immunocytochemistry (ICC). AhR expression was reduced in GNPs from Ahr CKO mice, compared to controls (Fig. 2B). Body and brain weights were not different between Ahr CKO and control mice (data not shown). These results indicate that Math1-mediated Cre recombinase excision of AhR alleles led to reduced AhR protein levels in GNPs, and establishes our model to study the impact of AhR expression on cerebellar granule neuron development.

Cerebellar DNA content is diminished during postnatal development in AhR CKO mice

Our previous studies indicate that global loss of AhR expression reduced adult mouse cerebellar DNA content, which serves as a surrogate method to estimate cell number (Collins *et al.*, 2008 and Labarca and Paigen, 1980). However, because every cell lacked AhR expression, we were unable to ascertain a cell autonomous role for AhR in granule neuron development. To determine whether AhR activity is required in GNPs to generate normal numbers of granule neurons, we analyzed DNA content in whole cerebella from AhR CKO and control mice. DNA content did not differ among the several animal control constructs, including $AhR^{wt/wt}$, $AhR^{fx/fx}$, and $AhR^{+/+}$/$Math1^{Cre/+}$ cerebella at PND60, indicating that neither floxed AhR alleles nor Cre recombinase expression in GNPs alone impacts cerebellar cell numbers (data not shown). In contrast, cerebellar DNA content was significantly reduced in AhR CKO mice during multiple developmental stages including PND10, 21, and 60 (Fig. 3A-C). Interestingly, the percent reduction increased as the animals aged from PND10 (17%), to PND21 (20%), to PND60 (23%), suggesting that cell depletion may be a progressive phenomenon in our model. Therefore, DNA content was analyzed from 9-12 month old mice. Nearly statistically significant (p=0.06), DNA content was reduced at 9-12 months by 34% in AhR CKO mice, compared to controls (Fig. 3D).

Reduced numbers of cerebellar granule neurons reside in the internal granule layer (IGL) of AhR CKO mice

Our findings suggest that AhR expression in GNPs impacts adult cerebellar cell number, and the foregoing time course analysis suggests effects occur early, during precursor proliferation, migration and differentiation. To define the effects of AhR deletion on proliferation and survival, we injected 50 mg/kg bromodeoxyuridine (BrdU) on PND10 because our AhR ICC data from figure 2B showed reduced AhR expression in Ahr CKO, and then analyzed cerebella from AhR CKO and control mice later, at PND21 and PND60. Fluorescence immunohistochemistry was used to track the fate of cells that incorporated BrdU injected at PND10. In cerebella lacking AhR in GNPs, there were 35% fewer BrdU positive cells that reached the internal granule layer (IGL), the final destination of these

cells, compared to GNPs with competent AhR expression (Fig. 4A). Interestingly, adult AhR CKO cerebella also had 37% fewer BrdU labeled cells that migrated to the IGL, compared to control (Fig. 4B). These results suggest that fewer mature granule neurons reach the IGL in adult mice following reduction of AhR in GNPs, findings consistent with the reductions in DNA content observed during postnatal development (Fig. 3).

AhR deletion leads to reduced numbers of GNPs in the S and G_2/M phases of the cell cycle without affecting survival

One mechanism that may contribute to reduced total cells as well as numbers of mature granule neurons in the IGL would be a changes in the cell cycle. To address this issue, we investigated the numbers of GNPs in the S and G_2/M phases of the cell cycle, using BrdU and phosphorylated histone 3 (pH3) IHC, respectively. There was a 25% decrease in the proportion of BrdU labeled cells in the EGL of mice lacking AhR in their GNPs (Fig. 5A-C). Moreover, there was a 25% decrease in the number of pH3 positive cells in the AhR CKO (Fig. 5D-E), suggesting that there were fewer mitoses. As an alternative mechanism, there may have been an increase in cell death. However, we did not detect any difference in the number of apoptotic cells using the TUNEL assay, suggesting cell death was not affected following AhR excision (5F-G). These data imply that proliferation of GNPs is reduced when AhR is genetically deleted.

Our *in vivo* data suggest that AhR expression in GNPs positively influences mature cerebellar granule cell number, possibly through controlling GNP cell cycle activity in the EGL during the postnatal expansion phase. To further test this hypothesis, we incubated GNPs in proliferative media and used ^{3}H-thymidine incorporation as a means to measure DNA synthesis *in vitro,* a marker for cells engaged in S phase. GNPs from the AhR CKO incorporated 13% less ^{3}H-thymidine when cultured in the presence of 10% serum (Fig. 6A). Furthermore, when incubated in defined medium containing the GNP mitogen, Shh (Weschler-Reya and Scott, 1999), there was also a 25% decrease in ^{3}H-thymidine incorporation (Fig. 6), suggesting this proliferative deficiency was not dependent on undefined serum factors. On the other hand, AhR CKO GNP cell survival was not affected compared to control cells (6B). These results suggest that the AhR is a positive regulator of GNP cell DNA synthesis and may serve to control the transition from proliferation to differentiation.

AhR deletion leads to enhanced GNP differentiation

As the foregoing data suggests AhR normally maintains GNP proliferation, its absence may be expected to impact cellular differentiation as well. To explore this possibility, GNPs from AhR CKO and control mice were incubated without mitogenic factors in order to promote differentiation and neurite outgrowth was measured using immunocytochemistry for βIII-tubulin expression, a cytoskeletal protein localized to differentiating neurons (Przyborski and Cambray-Deakin, 1997). The GNPs from AhR CKO mice elaborated more neurites compared to controls (Fig. 7A). There was a 34% increase in neurite outgrowth after 24hr *in vitro* (Fig. 7B). Because we cultured GNPs as aggregates, it may be difficult to distinguish fasciculated neurites from individual neurites. Therefore, to get a more accurate readout of GNP differentiation with and without AhR expression, we performed low-density GNP

cultures and transduced them with a lentivirus encoding a previously identified AhR shRNA that targets the murine transcript for degradation. Following 72 hrs of differentiation and puromycin selection of positively transduced cells, we observed a 40% increase in neurite outgrowth when AhR was knockdown (Fig. 7C). Collectively, these data suggest that an AhR deficiency in GNPs promotes differentiation. Together with the effects on DNA synthesis, these observations suggest that in the absence of AhR, GNP transition from proliferation to differentiation.

GABAR $_{A\alpha6}$ is elevated in the adult cerebellum following AhR deletion

Given that cell autonomous deletion of AhR in GNPs resulted in enhanced neurite outgrowth in culture, we wondered whether granule neuron differentiation may also exhibit changes *in vivo*, where their development is significantly influenced by neighboring Purkinje cells, astrocytes and oligodendrocytes (Hatten and Heintz, 1995). Therefore, we performed immunohistological analysis of $GABAR_{A\alpha6}$, a marker for mature granule neurons. In addition, we also explored the other possibility, that changes in GNP may impact interacting Purkinje neurons, which express calbindin. Representative images (Fig. 8A) suggest there is no major cytoarchitectural change in folia development, nor Purkinje cell localization. However, qualitatively, there seemed to be an increase in $GABAR_{A\alpha6}$ intensity. To quantify this, we performed immunoblot analysis of whole cerebellar protein extracts for $GABAR_{A\alpha6}$ expression from AhR CKO and control mice. There was a 33% increase in adult cerebellar $GABAR_{A\alpha6}$ expression in the absence of AhR compared to controls (Fig. 8B). In contrast, there was no change in calbindin protein levels, suggesting that effects were specific to granule neurons (Fig. 8C). We also investigated the distribution patterns of astrocytes and oligodendrocytes, using glial fibrillary acidic protein (GFAP) and myelin basic protein (MBP), respectively, and found no apparent differences between genotypes (data not shown).

Granule neuron precursor cell cycle related genes are altered in AhR CKO mice throughout early postnatal development

Since the AhR is a transcription factor suspected to regulate cell cycle related genes in a variety of tissues, including the CNS, we reasoned that the significant decrease in GNP proliferation and increase in differentiation in AhR CKO mice was due the transcriptional activity of the Ah receptor. To that end, we performed RT-qPCR analysis on essential cell cycle and early differentiation transcripts from AhR CKO or wildtype mice at PND6, 8, and 15, which are the key stages of murine GNP proliferation, differentiation, and migration (Roussel and Hatten, 2011). Our transcript analyses specifically focused on the GNP cell cycle activators (Atoh1, Hesx1, cyclin d5), the cell cycle inhibitors (p57, cdkn18), and the pro differentiators (cntn2, Neuro D). Collectively, there was a trend towards a decrease in cell cycle related genes at PND8 and an increase at PND15 in AhR CKO GNPs, implicating dysregulation of proliferation and/or early differentiation/cell cycle exit transcriptional programs. Interestingly, there was a three fold increase in Atoh1 at PND15 GNPs, which might indicate an AhR repressor target, or that there are AhR-independent compensatory changes occurring to increase CGN cell number in the IGL. Nevertheless, future studies are necessary to discriminate between bona fide AhR transcriptional targets and secondary/compensatory signaling effects following AhR removal.

DISCUSSION

Our observations indicate that when AhR is deleted specifically in GNPs, fewer cells proliferate, as evidenced by decreases in S-phase and M-phase markers and DNA synthesis, as well as reductions in total cerebellar cells and IGL neurons. Furthermore, GNP differentiation is enhanced, with GNPs growing more neurites and cells expressing increased levels of $GABAR_{A\alpha 6}$ protein. These results emerging from GNP-specific deletion of AhR are consistent with our prior studies in which there was global disruption of AhR functions. Previously, we found that the AhR is highly expressed and transcriptionally active in GNPs both *in vivo* and *in vitro* (Williamson *et al.*, 2005). Activation of AhR with TCDD, the potent environmental toxicant, disrupted GNP proliferation and differentiation during the critical period of postnatal development, presumably through sequestration of AhR from endogenous regulatory functions (Collins *et al.*, 2008). Furthermore, cerebella from adult $AhR^{-/-}$ mice had reduced cell numbers and exhibited abnormal differentiation of GNPs into mature neurons (Collins *et al.*, 2008). These previous observations suggested that the AhR serves an intrinsic function in GNP maturation, which is disrupted by TCDD exposure or its deletion. We have now tested the hypothesis that the AhR plays a cell-autonomous role in GNP proliferation and differentiation during cerebellar development, by creating a GNP-specific AhR knockout mouse, using the Cre/LoxP conditional knockout strategy. Overall, our findings suggest that loss of AhR in GNPs dysregulates neurogenesis, resulting in fewer mature cerebellar granule neurons in the IGL. Collectively, our data led us to speculate that AhR controls the timing between proliferation and differentiation, potentially by maintaining GNPs in their cycling state.

The AhR has been shown previously to regulate the cell cycle, acting through checkpoint regulatory proteins at the G_1/S or G_2/M boundaries (Gasiewicz *et al.*, 2008). Specifically, AhR was reported to promote p300-mediated induction of DNA synthesis, via its transcriptional domain (Tohkin *et al.*, 2000). In addition, mouse embryonic fibroblasts from $AhR^{-/-}$ mice exhibited slower growth and accumulation in the G_2/M phase of the cell cycle, which was accompanied by changes in the expression of the G_2/M kinases, Cdc2 and Plk (Elizondo *et al.*, 2000). Our laboratory has recently shown that AhR expression positively correlates with the proliferation of human medulloblastoma cells, thought to arise from abnormal proliferating GNPs, by modulating G_1/S cell cycle regulatory genes (Dever and Opanashuk, 2012). Moreover, AhR mRNA is highly expressed in the EGL during early murine postnatal development (Allen Brain Atlas). These findings suggest that the AhR has diverse roles in regulating cell cycle checkpoint genes, and thus modulating its activity would likely impact GNP cell cycle activity, as we now find. However, the role of AhR in regulating the timing of proliferation and cell cycle exit in GNPs remains unclear. In this study, we showed that AhR excision specifically in GNPs resulted in fewer cells in the S-phase of the cell cycle *in vivo* and *in vitro*. Furthermore, there were fewer cells in the G_2/M phase, as evidenced by reduced numbers of pH3 positive GNPs in the EGL following AhR deletion. These observations imply that AhR is promoting the proliferation of GNPs by regulating either G_1/S and/or G_2/M entry and is consistent with our previously published data showing that TCDD-induced sequestration of AhR induces cell cycle arrest through receptor downregulation (Williamson *et al.*, 2005). However, there are two questions that

remain to be addressed in future studies: 1) Are AhR-deficient GNPs cycling slower, exiting the cell cycle earlier, or dying? 2) By which mechanism(s) is AhR producing these cell cycle perturbations? Our data do not support enhanced cell death of GNP in the absence of AhR, neither *in vivo* nor *in vitro*. Interestingly, our Q-PCR analyses indicate dysregulated GNP cell cycle regulators following AhR removal, suggesting that future cell cycle and transcriptional profiling studies are warranted to identify bona fide AhR transcriptional targets. It is also possible that AhR deficient GNPs are cycling slower and/or differentiating earlier.

AhR activity has been associated with modulating the differentiation of both neural and non-neural cells (Gasiewicz *et al.*, 2008). Previously we found that neurite outgrowth was increased in GNPs isolated from global AhR null mice compared to wild type cells *in vitro* (Collins *et al.*, 2008). In this study we investigated the differentiation of GNPs in our cell specific AhR genetic deletion model. After 24 hours of differentiation *in vitro*, GNP aggregates devoid of AhR expression elaborated more neurites compared to wildtype cells, as measured by βIII-tubulin patterning. Furthermore, when we culture GNPs as single cells, there was a 40% increase in the number of neurites per GNP following lentiviral-mediated shRNA knockdown of AhR *in* vitro. Collectively, these data suggest that AhR expression negatively influences GNP differentiation in a cell autonomous manner. Because bHLH proteins are known to interact with each other to facilitate biological events, it is possible that AhR modulates bHLH expression and/or activity to inhibit GNP differentiation. For example, Hes1, another evolutionarily conserved bHLH protein member and a described AhR target gene (Thomsen *et al.*, 2004), was reported to be highly expressed in proliferating GNPs (Solecki *et al.*, 2001). Furthermore, Hes1 overexpression was previously shown to inhibit GNP differentiation and neurite outgrowth, suggesting it can suppress cell cycle exit genes (Solecki *et al.*, 2001). Our preliminary transcript analyses shows that Hes1 expression may be reduced at PND8 and increased at PND15 in AhR CKO GNPs, indicating loss of AhR influences Hes1 expression, either directly or indirectly. It is also possible that the AhR promotes the cycling of GNPs by inhibiting cell cycle exit and differentiation genes, potentially via modulating Hes1 expression; however, a direct link between AhR, Hes1, and GNP differentiation remains undefined and is of interest for future studies. Given our data related to cell division and maturation, it is conceivable that AhR could be important for balancing the transition between GNP proliferation and maturation. Consequently, affecting the timing of GNP maturation into granule neurons in IGL could have implications for cerebellar granule cell survival.

Normal programmed cell death, or apoptosis, is required to maintain proper cerebellar cytoarchitecture during development. Approximately half of GNPs in the rodent cerebellum undergo apoptosis, with the peak period of apoptosis in mice being around PND10 (White and Barone, 2001; Mooney and Miller, 2000). The AhR has been implicated to promote apoptosis in neuronal and non-neuronal cells, albeit via activation by exposure to exogenous ligands, such as TCDD and β-Naphthoflavone (Kajta *et al.*, 2009 and Ivnitski *et al.*, 2001). In addition, our DNA content studies show that there may be a progressive loss of cells throughout development, suggesting that a decline in cell birth may not be the only mechanism contributing to the reduction of granule neurons in the adult AhR CKO cerebellum. Therefore, we investigated whether the reduction of granule neurons in the adult

cerebellum resulted from increased apoptosis during early postnatal development. However, there were no differences in the numbers of apoptotic cells in the EGL or ML/IGL in AhR CKO mice. We also did not observe viability changes *in vitro.* There is a second wave of apoptosis that peaks at PND21 in the developing cerebellum, so it is possible that we missed the window where there was a difference in the number of apoptotic cells (White and Barone, 2001). However, a reduction in Brd-U positive GNPs was seen well before PND21, suggesting that cell birth, and not cell death, was the primary reason for reduced cerebellar granule neurons in the IGL. Further examination of adult AhR CKO cerebellar tissue indicated an increase in $GABAR_{A\alpha6}$ expression, which is restricted to terminally differentiated granule neurons in the IGL of the developing mouse cerebellum (Zheng *et al.*, 1993). These findings may suggest there is a compensatory increase in $GABAR_{A\alpha6}$ expression in the IGL due to the reduction of GNP cell births in the EGL, though more direct effects on differentiation programs by this bHLH transcription factor cannot be excluded.

Recent studies have shown a relationship between AhR expression/activity and CNS development. Invertebrate orthologs of AhR participate in neural cell fate decisions, differentiation, migration, and dendrite growth during neurogenesis (Huang *et al.*, 2004; Qin and Powell-Coffman, 2004; Kim *et al.*, 2006). Moreover, studies from our laboratory suggest that AhR participates in diverse regions of ongoing neurogenesis including the embryonic forebrain, the postnatal cerebellum and the adult hippocampus (Collins *et al.*, 2008 and Latchney *et al.,* 2013). This information supports the idea that the AhR has an evolutionarily conserved role during neurogenesis. Because AhR is also a xenobiotic responsive protein, it implies that abnormal activation of AhR via exogenous ligands, such as TCDD or dioxin-like compounds, could influence cerebellar granule cell neurogenesis and function by diverting AhR from its endogenous roles. Because exogenous and endogenous ligands usually have affinities in the nanomolar range and micromolar range, respectively, it is conceivable that TCDD and/or dioxin-like exposure would displace endogenous ligands, abnormally activating AhR-mediated genetic programs (Denison and Nagy, 2003). Accordingly, various developmental abnormalities, consistent with atypical cerebellar development, have been observed following perinatal exposure to TCDD and dioxin-like compounds, which implicates the cerebellum as a target for AhR-induced neurotoxicity (Thiel *et al.*, 1994; Schantz, 1996; Kakeyama and Tohyama, 2003). However, these studies were not able to ascertain the precise cellular targets of TCDD toxicity. Our observations now provide insight into the potential consequences of abnormal activation of AhR in granule cells by exogenous ligands found in the environment.

This study tested the hypothesis that the AhR has an endogenous role in the generation and maturation of cerebellar granule cells. Our results indicate that loss of AhR in GNPs negatively impacted final granule neuron numbers, possibly through the cell-autonomous pro-proliferative role of AhR in GNPs. Based on the observations, the hypothesis that the AhR maintains the GNP pool by promoting cell cycle activity and restricting differentiation is favored. Humans are regularly exposed to AhR agonists and antagonists through diet and inhalation (Schecter *et al.*, 2001). Consequently, untimely or sustained AhR activation through exogenous ligands in GNPs could contribute to the formation of a variety of developmental cerebellar disorders, such as medulloblastoma, a primary cerebellar tumor

thought to arise from abnormal cycling GNPs (Wechsler-Reya and Scott, 2001; Roussel and Hatten, 2011). Our laboratory recently published results describing AhR as a pro-proliferative protein in human medulloblastoma cells (Dever and Opanashuk, 2012). However, future mechanistic studies are necessary to understand if TCDD or dioxin-like compounds are a risk factor for medulloblastoma pathogenesis. These studies provide novel insights for understanding the endogenous roles of AhR signaling during cerebellar granule cell development, and may have significant implications for the effects of environmental factors in cerebellar dysgenesis.

Acknowledgments

This research was supported by the National Institutes of Health (R01 ES016357, P30 ES01247, and T32 ES07026). We would like to acknowledge Carrie Klocke for her assistance in the laboratory.

REFERENCES

Allen Institute for Brain Science. Allen Brain Atlas [Internet]. Available from: http://www.brain-map.org.

Aruga J, Inoue T, Hoshino J, Mikoshiba K. Zic2 controls cerebellar development in cooperation with Zic1. The Journal of neuroscience : the official journal of the Society for Neuroscience. 2002; 22:218–225. [PubMed: 11756505]

Behesti H, Marino S. Cerebellar granule cells: insights into proliferation, differentiation, and role in medulloblastoma pathogenesis. The international journal of biochemistry & cell biology. 2009; 41:435–445. [PubMed: 18755286]

Ben-Arie N, McCall AE, Berkman S, Eichele G, Bellen HJ, Zoghbi HY. Evolutionary conservation of sequence and expression of the bHLH protein Atonal suggests a conserved role in neurogenesis. Human molecular genetics. 1996; 5:1207–1216. [PubMed: 8872459]

Birnbaum LS, Tuomisto J. Non-carcinogenic effects of TCDD in animals. Food additives and contaminants. 2000; 17:275–288. [PubMed: 10912242]

Cheng Y, Tao Y, Black IB, DiCicco-Bloom E. A single peripheral injection of basic fibroblast growth factor (bFGF) stimulates granule cell production and increases cerebellar growth in newborn rats. Journal of neurobiology. 2001; 46:220–229. [PubMed: 11169507]

Collins LL, Williamson MA, Thompson BD, Dever DP, Gasiewicz TA, Opanashuk LA. 2,3,7,8-Tetracholorodibenzo-p-dioxin exposure disrupts granule neuron precursor maturation in the developing mouse cerebellum. Toxicol Sci. 2008; 103:125–136. [PubMed: 18227101]

Corrales JD, Blaess S, Mahoney EM, Joyner AL. The level of sonic hedgehog signaling regulates the complexity of cerebellar foliation. Development. 2006; 133:1811–1821. [PubMed: 16571625]

Crews ST. Control of cell lineage-specific development and transcription by bHLH-PAS proteins. Genes Dev. 1998; 12:607–620. [PubMed: 9499397]

Crews ST, Fan CM. Remembrance of things PAS: regulation of development by bHLH-PAS proteins. Current opinion in genetics & development. 1999; 9:580–587. [PubMed: 10508688]

Denison MS, Nagy SR. Activation of the aryl hydrocarbon receptor by structurally diverse exogenous and endogenous chemicals. Annual review of pharmacology and toxicology. 2003; 43:309–334.

Dever DP, Opanashuk LA. The aryl hydrocarbon receptor contributes to the proliferation of human medulloblastoma cells. Molecular pharmacology. 2012; 81:669–678. [PubMed: 22311706]

Duman-Scheel M, Weng L, Xin S, Du W. Hedgehog regulates cell growth and proliferation by inducing Cyclin D and Cyclin E. Nature. 2002; 417:299–304. [PubMed: 12015606]

Elizondo G, Fernandez-Salguero P, Sheikh MS, Kim GY, Fornace AJ, Lee KS, Gonzalez FJ. Altered cell cycle control at the G(2)/M phases in aryl hydrocarbon receptor-null embryo fibroblast. Mol Pharmacol. 2000; 57:1056–1063. [PubMed: 10779392]

Gasiewicz TA, Henry EC, Collins LL. Expression and activity of aryl hydrocarbon receptors in development and cancer. Critical reviews in eukaryotic gene expression. 2008; 18:279–321. [PubMed: 18652561]

Goodlett CR, Hamre KM, West JR. Dissociation of spatial navigation and visual guidance performance in Purkinje cell degeneration (pcd) mutant mice. Behavioural brain research. 1992; 47:129–141. [PubMed: 1590945]

Gu YZ, Hogenesch JB, Bradfield CA. The PAS superfamily: sensors of environmental and developmental signals. Annual review of pharmacology and toxicology. 2000; 40:519–561.

Hatten ME, Heintz N. Mechanisms of neural patterning and specification in the developing cerebellum. Annual review of neuroscience. 1995; 18:385–408.

Hatten ME, Alder J, Zimmerman K, Heintz N. Genes involved in cerebellar cell specification and differentiation. Current opinion in neurobiology. 1997; 7:40–47. [PubMed: 9039803]

Huang X, Powell-Coffman JA, Jin Y. The AHR-1 aryl hydrocarbon receptor and its co-factor the AHA-1 aryl hydrocarbon receptor nuclear translocator specify GABAergic neuron cell fate in C. elegans. Development. 2004; 131:819–828. [PubMed: 14757639]

Ivnitski I, Elmaoued R, Walker MK. 2,3,7,8-tetrachlorodibenzo-p-dioxin (TCDD) inhibition of coronary development is preceded by a decrease in myocyte proliferation and an increase in cardiac apoptosis. Teratology. 2001; 64:201–212. [PubMed: 11598926]

Kajta M, Wojtowicz AK, Mackowiak M, Lason W. Aryl hydrocarbon receptor-mediated apoptosis of neuronal cells: a possible interaction with estrogen receptor signaling. Neuroscience. 2009; 158:811–822. [PubMed: 19027052]

Kakeyama M, Tohyama C. Developmental neurotoxicity of dioxin and its related compounds. Industrial health. 2003; 41:215–230. [PubMed: 12916752]

Kenney AM, Rowitch DH. Sonic hedgehog promotes G(1) cyclin expression and sustained cell cycle progression in mammalian neuronal precursors. Molecular and cellular biology. 2000; 20:9055–9067. [PubMed: 11074003]

Kenney AM, Cole MD, Rowitch DH. Nmyc upregulation by sonic hedgehog signaling promotes proliferation in developing cerebellar granule neuron precursors. Development. 2003; 130:15–28. [PubMed: 12441288]

Kenney AM, Widlund HR, Rowitch DH. Hedgehog and PI-3 kinase signaling converge on Nmyc1 to promote cell cycle progression in cerebellar neuronal precursors. Development. 2004; 131:217–228. [PubMed: 14660435]

Kim MD, Jan LY, Jan YN. The bHLH-PAS protein Spineless is necessary for the diversification of dendrite morphology of Drosophila dendritic arborization neurons. Genes Dev. 2006; 20:2806–2819. [PubMed: 17015425]

Labarca C, Paigen K. A simple, rapid, and sensitive DNA assay procedure. Analytical biochemistry. 1980; 102:344–352. [PubMed: 6158890]

Lahvis GP, Pyzalski RW, Glover E, Pitot HC, McElwee MK, Bradfield CA. The aryl hydrocarbon receptor is required for developmental closure of the ductus venosus in the neonatal mouse. Mol Pharmacol. 2005; 67:714–720. [PubMed: 15590894]

Latchney SE, Hein AM, O'Banion MK, DiCicco-Bloom E, Opanashuk LA. Deletion or activation of the aryl hydrocarbon receptor alters adult hippocampal neurogenesis and contextual fear memory. Journal of neurochemistry. 2013; 125:430–445. [PubMed: 23240617]

Lee DW, Notter SA, Thiruchelvam M, Dever DP, Fitzpatrick R, Kostyniak PJ, Cory-Slechta DA, Opanashuk LA. Subchronic polychlorinated biphenyl (Aroclor 1254) exposure produces oxidative damage and neuronal death of ventral midbrain dopaminergic systems. Toxicological sciences : an official journal of the Society of Toxicology. 2012; 125:496–508. [PubMed: 22094459]

Loukas CG, Wilson GD, Vojnovic B, Linney A. An image analysis-based approach for automated counting of cancer cell nuclei in tissue sections. Cytometry Part A : the journal of the International Society for Analytical Cytology. 2003; 55:30–42. [PubMed: 12938186]

Lumpkin EA, Collisson T, Parab P, Omer-Abdalla A, Haeberle H, Chen P, Doetzlhofer A, White P, Groves A, Segil N, Johnson JE. Math1-driven GFP expression in the developing nervous system of transgenic mice. Gene expression patterns : GEP. 2003; 3:389–395. [PubMed: 12915300]

Lund AK, Goens MB, Kanagy NL, Walker MK. Cardiac hypertrophy in aryl hydrocarbon receptor null mice is correlated with elevated angiotensin II, endothelin-1, and mean arterial blood pressure. Toxicology and applied pharmacology. 2003; 193:177–187. [PubMed: 14644620]

Machold R, Fishell G. Math1 is expressed in temporally discrete pools of cerebellar rhombic-lip neural progenitors. Neuron. 2005; 48:17–24. [PubMed: 16202705]

McMillan BJ, Bradfield CA. The aryl hydrocarbon receptor sans xenobiotics: endogenous function in genetic model systems. Molecular pharmacology. 2007; 72:487–498. [PubMed: 17535977]

Miyata T, Maeda T, Lee JE. NeuroD is required for differentiation of the granule cells in the cerebellum and hippocampus. Genes & development. 1999; 13:1647–1652. [PubMed: 10398678]

Miyazawa K, Himi T, Garcia V, Yamagishi H, Sato S, Ishizaki Y. A role for p27/Kip1 in the control of cerebellar granule cell precursor proliferation. The Journal of neuroscience : the official journal of the Society for Neuroscience. 2000; 20:5756–5763. [PubMed: 10908616]

Mooney SM, Miller MW. Expression of bcl-2, bax, and caspase-3 in the brain of the developing rat. Brain research Developmental brain research. 2000; 123:103–117. [PubMed: 11042339]

Murata K, Hattori M, Hirai N, Shinozuka Y, Hirata H, Kageyama R, Sakai T, Minato N. Hes1 directly controls cell proliferation through the transcriptional repression of p27Kip1. Mol Cell Biol. 2005; 25:4262–4271. [PubMed: 15870295]

Muzumdar MD, Tasic B, Miyamichi K, Li L, Luo L. A global double-fluorescent Cre reporter mouse. Genesis. 2007; 45:593–605. [PubMed: 17868096]

Nicot A, DiCicco-Bloom E. Regulation of neuroblast mitosis is determined by PACAP receptor isoform expression. Proceedings of the National Academy of Sciences of the United States of America. 2001; 98:4758–4763. [PubMed: 11296303]

Pool M, Thiemann J, Bar-Or A, Fournier AE. NeuriteTracer: a novel ImageJ plugin for automated quantification of neurite outgrowth. Journal of neuroscience methods. 2008; 168:134–139. [PubMed: 17936365]

Przyborski SA, Cambray-Deakin MA. Profile of glutamylated tubulin expression during cerebellar granule cell development in vitro. Brain research Developmental brain research. 1997; 100:133–138. [PubMed: 9174257]

Qin H, Powell-Coffman JA. The Caenorhabditis elegans aryl hydrocarbon receptor, AHR-1, regulates neuronal development. Developmental biology. 2004; 270:64–75. [PubMed: 15136141]

Roussel MF, Hatten ME. Cerebellum development and medulloblastoma. Current topics in developmental biology. 2011; 94:235–282. [PubMed: 21295689]

Rossman IT, Lin L, Morgan KM, Digiovine M, Van Buskirk EK, Kamdar S, Millonig JH, Dicicco-Bloom E. Engrailed2 modulates cerebellar granule neuron precursor proliferation, differentiation and insulin-like growth factor 1 signaling during postnatal development. Mol Autism. 2014; 5:9. [PubMed: 24507165]

Schantz SL. Developmental neurotoxicity of PCBs in humans: what do we know and where do we go from here? Neurotoxicology and teratology. 1996; 18:217–227. discussion 229-276. [PubMed: 8725628]

Schecter A, Cramer P, Boggess K, Stanley J, Papke O, Olson J, Silver A, Schmitz M. Intake of dioxins and related compounds from food in the U.S. population. Journal of toxicology and environmental health Part A. 2001; 63:1–18. [PubMed: 11346131]

Schmidt JV, Su GH, Reddy JK, Simon MC, Bradfield CA. Characterization of a murine Ahr null allele: involvement of the Ah receptor in hepatic growth and development. Proc Natl Acad Sci U S A. 1996; 93:6731–6736. [PubMed: 8692887]

Solecki DJ, Liu XL, Tomoda T, Fang Y, Hatten ME. Activated Notch2 signaling inhibits differentiation of cerebellar granule neuron precursors by maintaining proliferation. Neuron. 2001; 31:557–568. [PubMed: 11545715]

Thiel R, Koch E, Ulbrich B, Chahoud I. Peri- and postnatal exposure to 2,3,7,8-tetrachlorodibenzo-p-dioxin: effects on physiological development, reflexes, locomotor activity and learning behaviour in Wistar rats. Archives of toxicology. 1994; 69:79–86. [PubMed: 7717865]

Thomsen JS, Kietz S, Strom A, Gustafsson JA. HES-1, a novel target gene for the aryl hydrocarbon receptor. Mol Pharmacol. 2004; 65:165–171. [PubMed: 14722248]

Tohkin M, Fukuhara M, Elizondo G, Tomita S, Gonzalez FJ. Aryl hydrocarbon receptor is required for p300-mediated induction of DNA synthesis by adenovirus E1A. Molecular pharmacology. 2000; 58:845–851. [PubMed: 10999956]

Walisser JA, Glover E, Pande K, Liss AL, Bradfield CA. Aryl hydrocarbon receptor-dependent liver development and hepatotoxicity are mediated by different cell types. Proceedings of the National Academy of Sciences of the United States of America. 2005; 102:17858–17863. [PubMed: 16301529]

Wang JY, Del Valle L, Gordon J, Rubini M, Romano G, Croul S, Peruzzi F, Khalili K, Reiss K. Activation of the IGF-IR system contributes to malignant growth of human and mouse medulloblastomas. Oncogene. 2001; 20:3857–3868. [PubMed: 11439349]

Wang VY, Zoghbi HY. Genetic regulation of cerebellar development. Nature reviews Neuroscience. 2001; 2:484–491. [PubMed: 11433373]

Wechsler-Reya RJ, Scott MP. Control of neuronal precursor proliferation in the cerebellum by Sonic Hedgehog. Neuron. 1999; 22:103–114. [PubMed: 10027293]

Wechsler-Reya R, Scott MP. The developmental biology of brain tumors. Annual review of neuroscience. 2001; 24:385–428.

Williamson MA, Gasiewicz TA, Opanashuk LA. Aryl hydrocarbon receptor expression and activity in cerebellar granule neuroblasts: implications for development and dioxin neurotoxicity. Toxicol Sci. 2005; 83:340–348. [PubMed: 15537747]

White LD, Barone S Jr. Qualitative and quantitative estimates of apoptosis from birth to senescence in the rat brain. Cell death and differentiation. 2001; 8:345–356. [PubMed: 11550086]

Yang H, Xie X, Deng M, Chen X, Gan L. Generation and characterization of Atoh1-Cre knock-in mouse line. Genesis. 2010; 48:407–413. [PubMed: 20533400]

Ye P, Xing Y, Dai Z, D'Ercole AJ. In vivo actions of insulin-like growth factor-I (IGF-I) on cerebellum development in transgenic mice: evidence that IGF-I increases proliferation of granule cell progenitors. Brain research Developmental brain research. 1996; 95:44–54. [PubMed: 8873975]

Zheng T, Santi MR, Bovolin P, Marlier LN, Grayson DR. Developmental expression of the alpha 6 GABAA receptor subunit mRNA occurs only after cerebellar granule cell migration. Brain research Developmental brain research. 1993; 75:91–103. [PubMed: 8222213]

Zheng C, Heintz N, Hatten ME. CNS gene encoding astrotactin, which supports neuronal migration along glial fibers. Science. 1996; 272:417–419. [PubMed: 8602532]

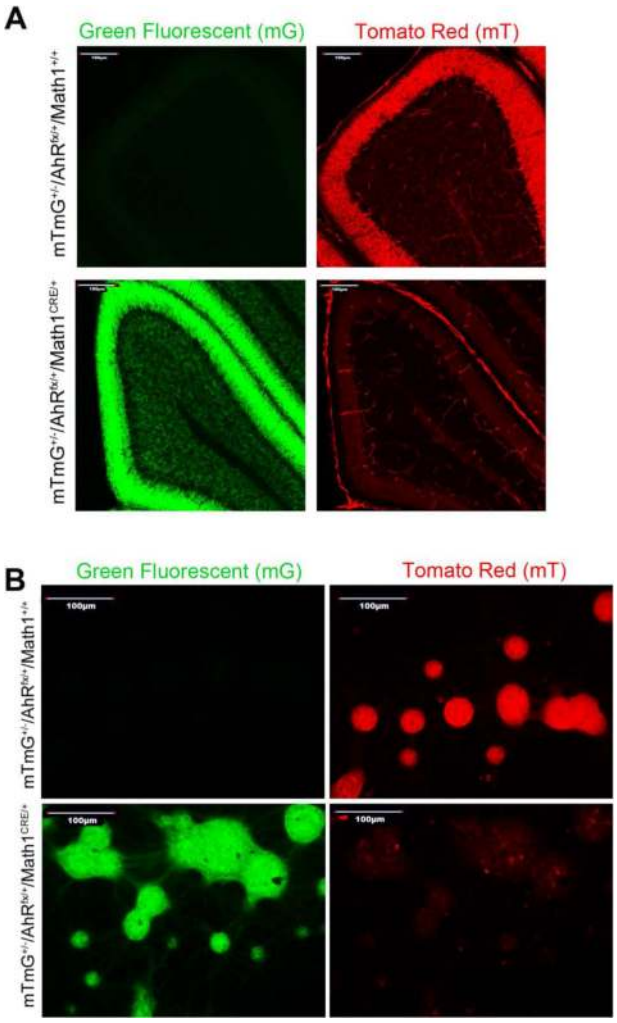

Fig 1. Cre recombinase is robustly expressed in cerebellar GNPs via the *Math1* promoter

mTmG/AhR$^{fx/+}$/Math1$^{+/+}$ and mTmG/AhR$^{fx/+}$/Math1$^{Cre/+}$ cerebella were harvested, fixed, and processed for detection of GFP and RFP. (**A)** Representative confocal images at 20×. *Top panels,* showing expression of mG and mT prior to recombination. *Bottom panels,* showing expression of mG and mT after Cre-mediation recombination. GFP visualization shows that Cre is highly expressed in EGL of the developing cerebellum. (**B)** GNPs isolated from AhR$^{fx/fx}$Math1$^{Cre/+}$ and AhR$^{fx/fx}$Math1$^{+/+}$ mice were cultured on poly-L-coated german-glass-coated coverslips for 24 hours, fixed, and analyzed for expression of mT and mG. Representative confocal images at 20× indicate that Cre recombinase activity is only observed in the Math1$^{Cre/+}$ GNPs (lower left panel) and is absent from those expressing Math1$^{+/+}$.

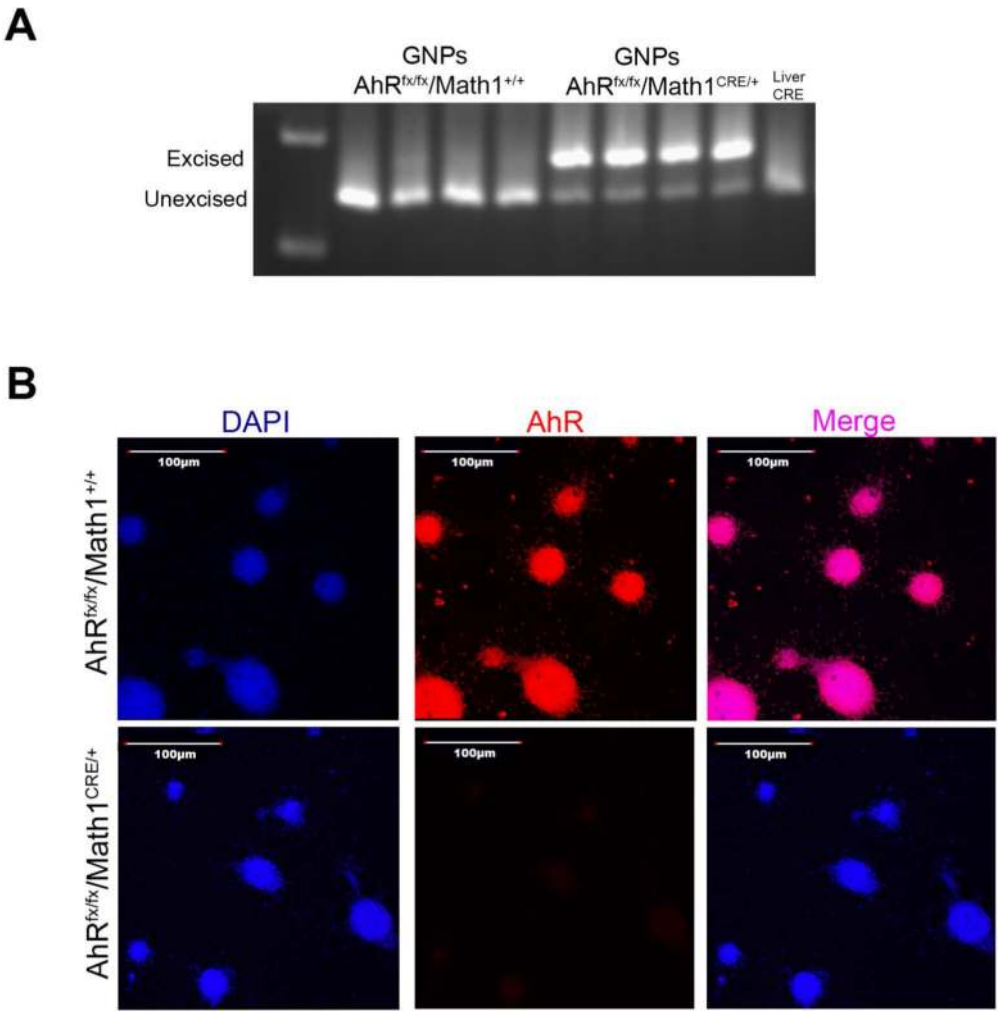

Fig 2. AhR expression is reduced in GNPs following *Math1*-mediated Cre recombination

$AhR^{fx/fx}Math1^{Cre/+}$ and $AhR^{fx/fx}Math1^{+/+}$ PND10 cerebella were harvested from 4 separate mice and processed for isolation of GNPs. (**A)** Genomic DNA was isolated and multiplex PCR was carried out to detect AhR excised and unexcised alleles. The AhR excised allele amplified an 180bp product, while the AhR unexcised allele generated a 140bp product (**B)** GNPs aggregates were grown on glass coverslips for 48hrs, fixed, and AhR expression was detected by immunofluorescence. Red=AhR; Blue=Dapi. Experiments were performed three times.

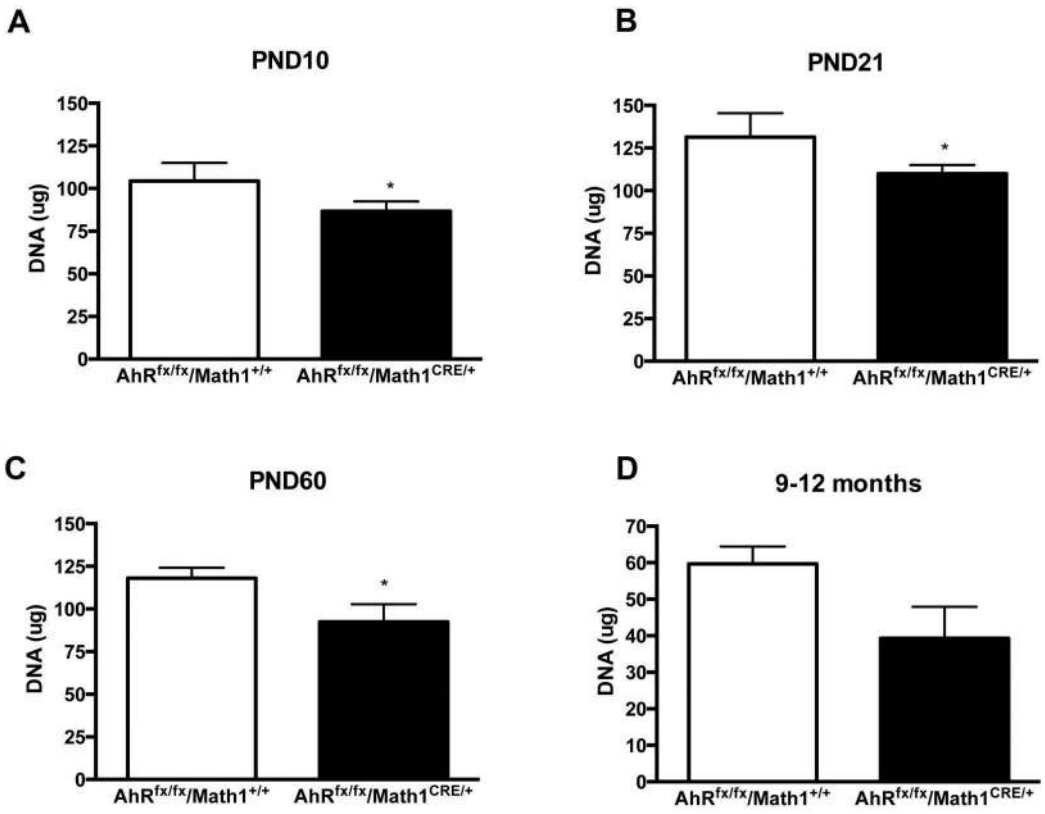

Fig 3. DNA content is diminished throughout postnatal development in AhR CKO mice

Cerebella tissue was collected from $AhR^{fx/fx}Math1^{Cre/+}$ and $AhR^{fx/fx}Math1^{+/+}$ mice at various time points throughout development. DNA content was measured using Hoechst 33258 and averages for each time point are reported in A-D. **(A)** PND10. **(B)** PND21. **(C)** PND60. **(D)** 9-12 months. Data represent mean +/- SEM (n=10 for each genotype at each age, *p<0.05, significantly different from $AhR^{fx/fx}Math1^{+/+}$, Student's t-test).

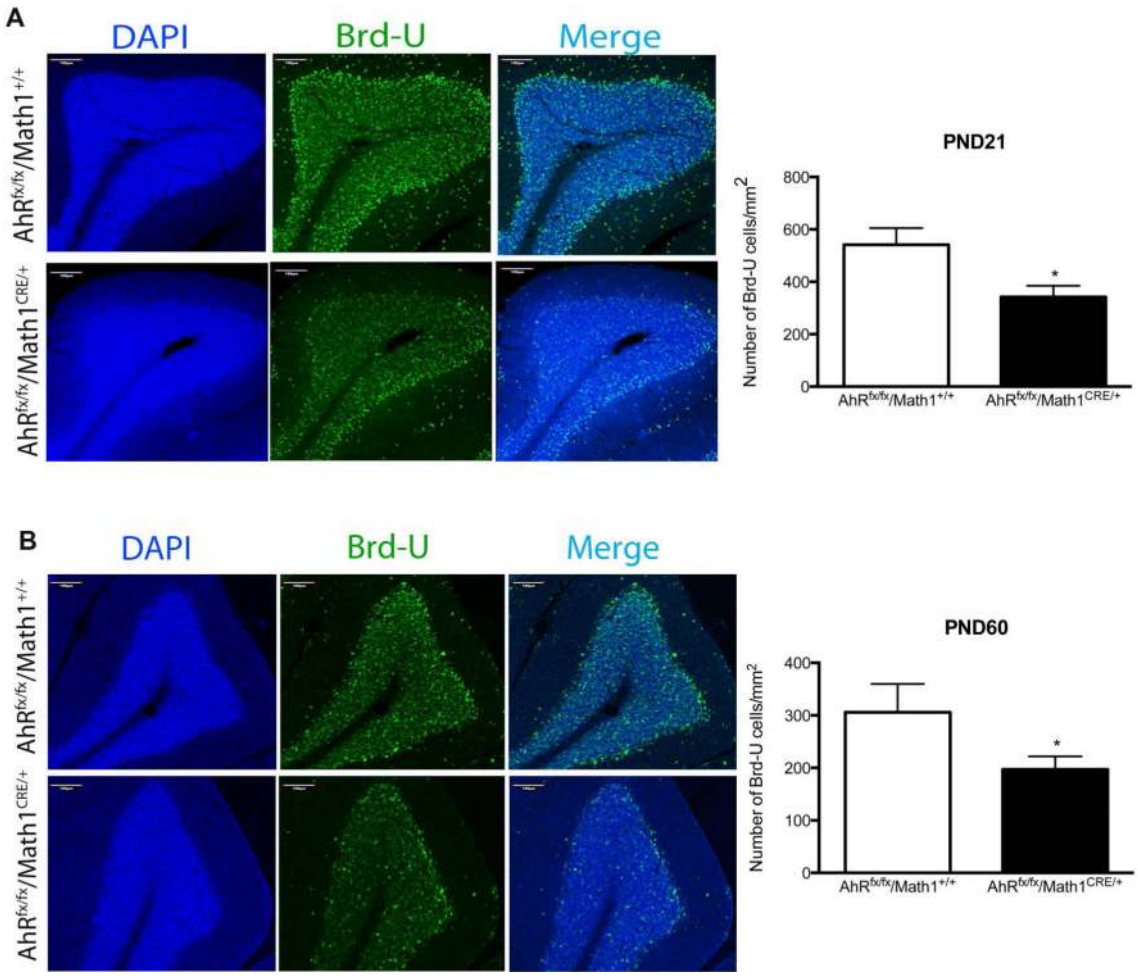

Fig 4. Reduced numbers of proliferating cerebellar granule neuron precursors from P10 later reside in the adult internal granule layer (IGL) of AHR CKO mice

$AhR^{fx/fx}Math1^{Cre/+}$ and $AhR^{fx/fx}Math1^{+/+}$ mice were administered BrdU (50 mg/kg) on PND10. Following perfusion at various developmental ages, mice were processed for the immunohistochemical detection of BrdU positive cells in the cerebellum. (**A)** PND21 mice (**B)** PND60 cerebella Figures show representative confocal images at 20×. BrdU=green; Dapi=blue. BrdU positive cells (green) were counted from 4-6 different sections of folia III per n, using ImageJ software. Data represent mean +/− SEM (n=5, *p<0.05, significantly different from $AhR^{fx/fx}Math1^{+/+}$, Student's t-test).

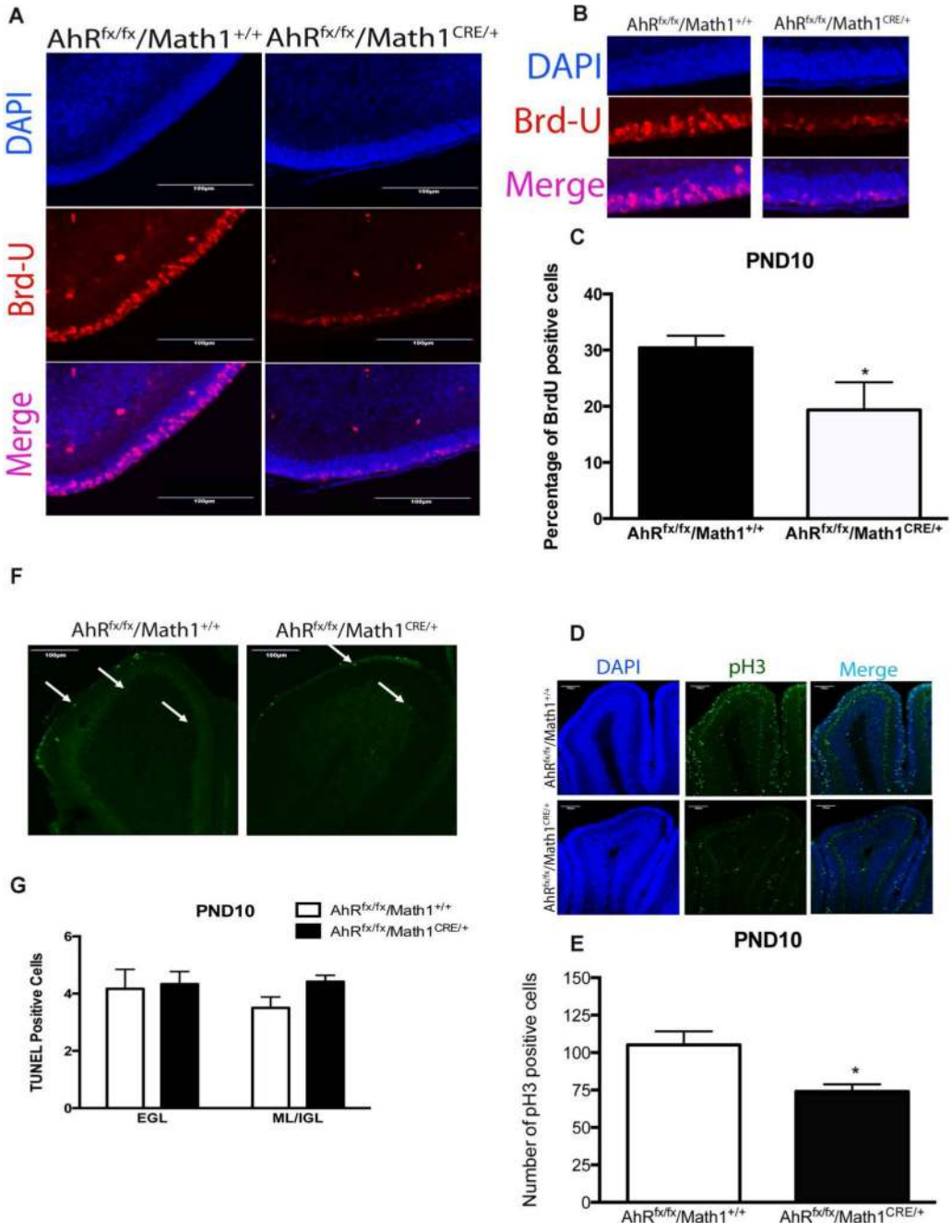

Fig 5. Reduced numbers of GNPs in the S and G_2/M phases of the cell cycle in the EGL following AhR deletion

Cerebella tissue, collected from $AhR^{fx/fx}Math1^{Cre/+}$ and $AhR^{fx/fx}Math1^{+/+}$ mice, was fixed and processed for immunohistochemical staining at PND10. (**A)** BrdU image at 20×. (**B**) BrdU image at 40×. **(C)** Quantification of number of BrdU positive cells in the EGL. **(D)** pH3 images at 10× cell cycle **(E)** Quantification of number of pH3 positive cells in the EGL. **(F)** TUNEL images at 20×. **(G)** Quantification of number of TUNEL positive cells in the EGL and ML/IGL. Brd-U positive cells (red), TUNEL positive cells (green), and pH3 positive cells (green) were counted from 4 different sections of folia III using ImageJ

software. Data represent mean +/− SEM (n=5 for BrdU and n=3 for TUNEL, *p<0.05, significantly different from $AhR^{fx/fx}Math1^{+/+}$, Student's t-test).

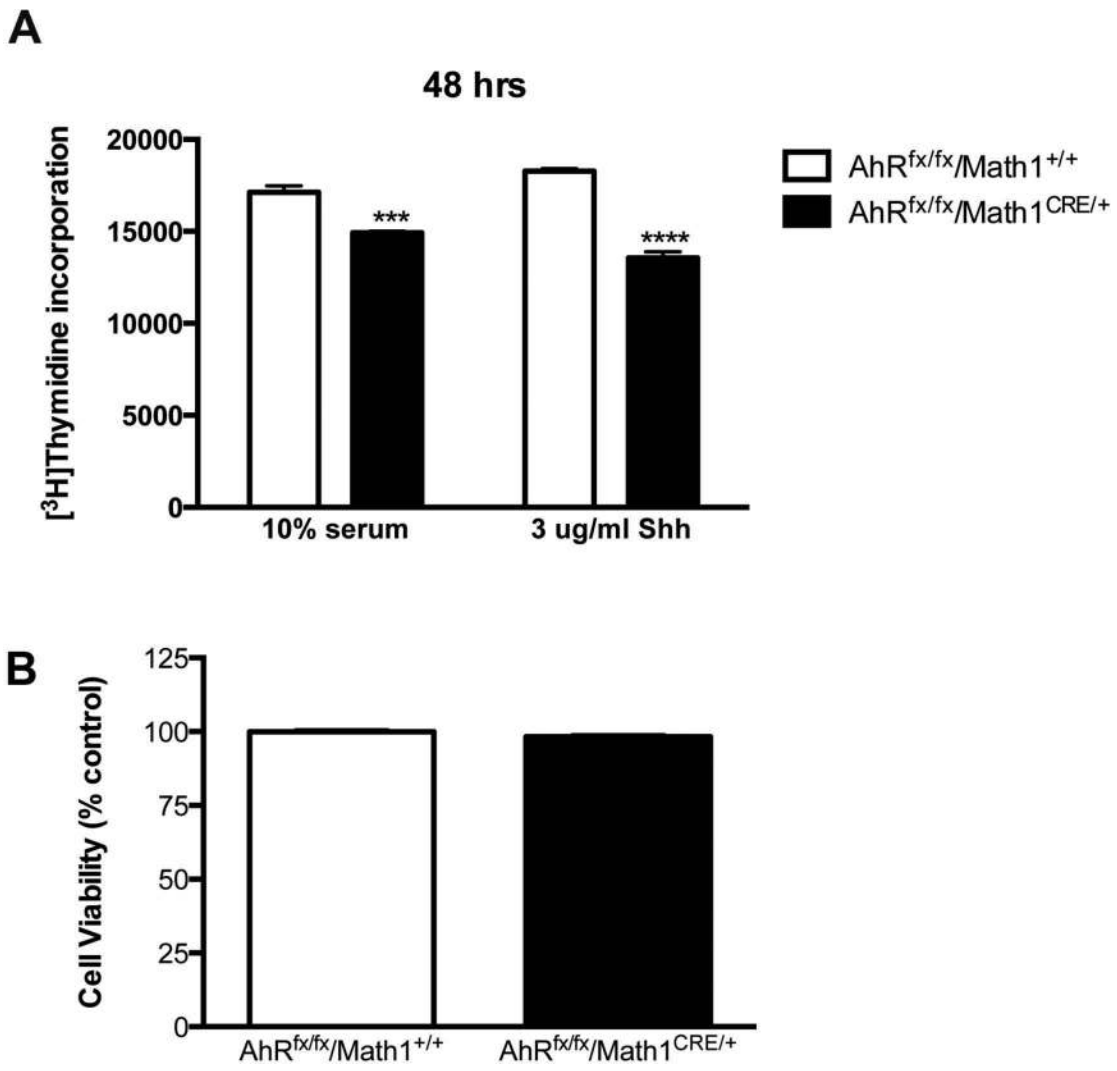

Fig 6. GNPs from AhR CKO mice incorporate less thymidine than controls

GNPs from AhR$^{fx/fx}$Math1$^{Cre/+}$ and AhR$^{fx/fx}$Math1$^{+/+}$ mice were aggregated for 48 hours in media with 10% serum or in defined medium containing 3μg/ml sonic hedgehog (Shh). (**A)** Cells were pulsed with 1μCi of methyl-^{3}H-thymidine at 24 hours and were assessed for incorporation at 48 hrs. (**B)** GNP aggregates at 48 hrs were incubated with MTS reagent for 4 hours at 37° C and absorbances were read at 490nm. Values are displayed as percent of control. Data represent mean +/− SEM (n=5, ***p<0.001, ****p<0.0001 significantly different from AhR$^{fx/fx}$Math1$^{+/+}$, two-way ANOVA). Graphs are representative of 3 independent experiments.

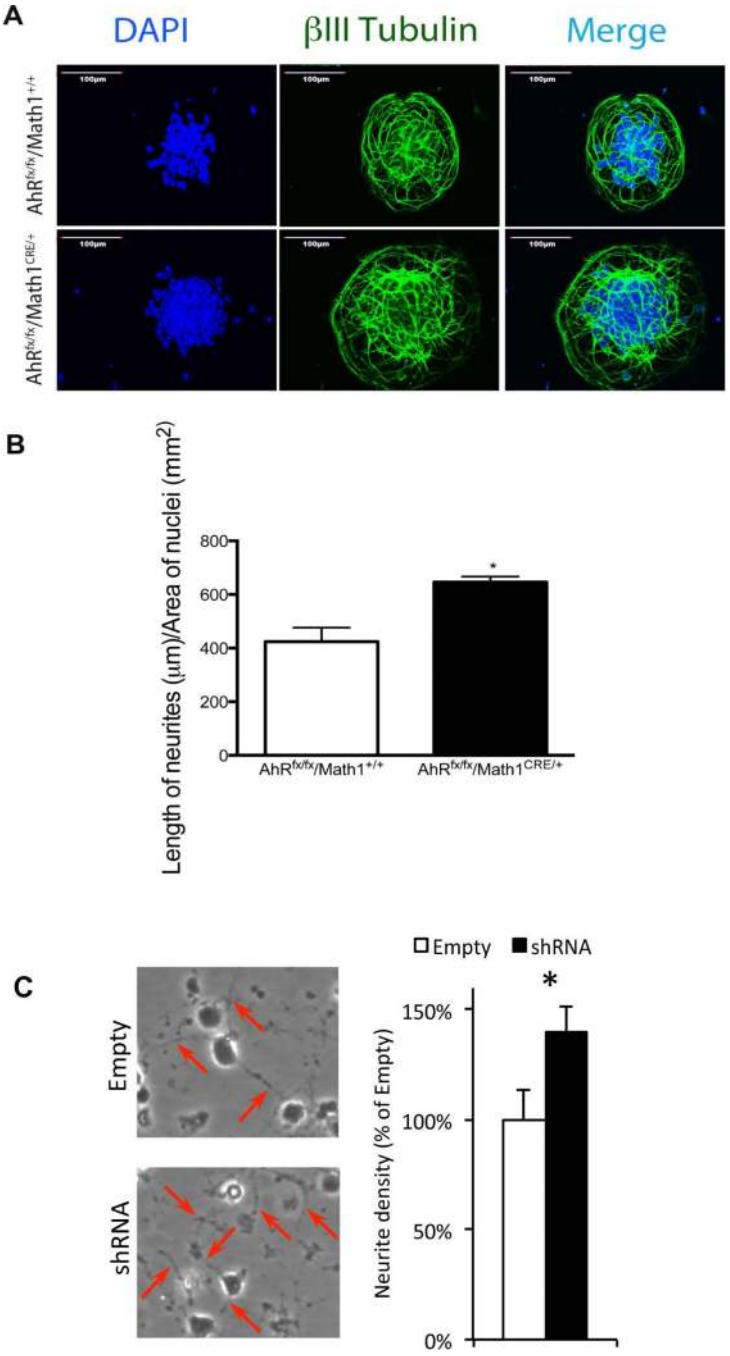

Fig 7. Neurite outgrowth is enhanced in GNPs from AhR CKO mice

(A) Granule neuroblast cultures were stained for β-III tubulin (green), as marker for neurite outgrowth, after 24 hours of differentiation *in vitro*. Overlay of images are shown. (**B)** Quantification was performed using ImageJ software. (C) On the left, representative images are shown of low-density single cell cultures transduced with a lentivirus encoding a non-targeting (Empty) or murine AhR targeting (shRNA) shRNA. Red arrows point toward typical neurites. On the right is the quantification of neurite density normalized with lived cells and expressed as % of empty via ImageJ software. Data represent mean +/− SEM (*n*=3,

*p<0.05, significantly different from $AhR^{fx/fx}Math1^{+/+}$, Student's *t*-test). Photomicrographs are representative of 3 independent experiments.

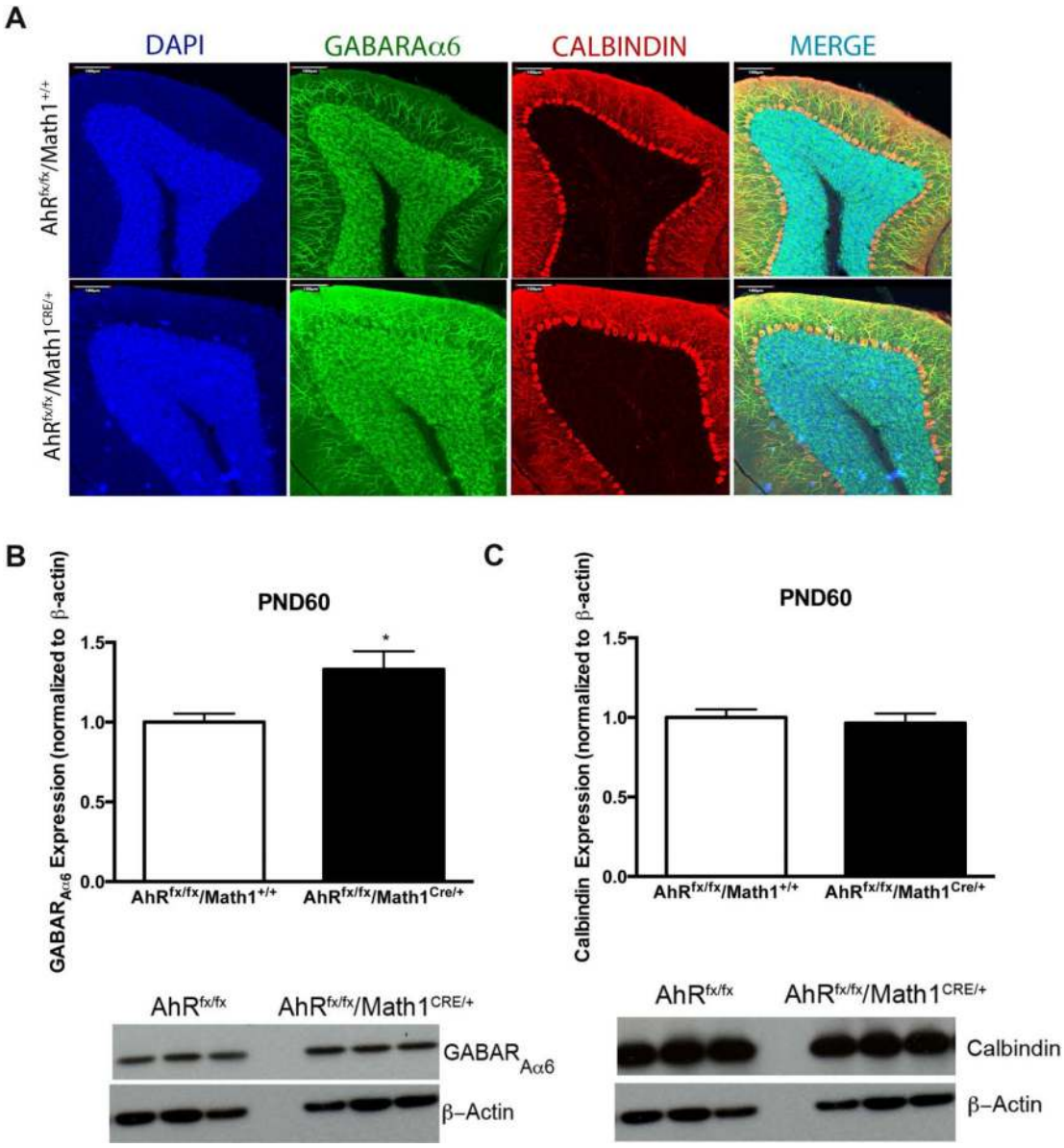

Fig 8. GABAR$_{Aα6}$ protein expression is increased in AhR deletion mutant cerebellum

(A) PND60 AhR$^{fx/fx}$Math1$^{Cre/+}$ and AhR$^{fx/fx}$Math1$^{+/+}$ mice were perfused and processed for histological analysis of calbindin and GABAR$_{Aα6}$ expression. Figures are representative confocal images at 20×. Dapi=blue; GABAR$_{Aα6}$=green; calbindin=red. (**B)** Protein (10μg) was separated by SDS-PAGE and then analyzed for GABAR$_{Aα6}$ expression via immunoblot. (**C)** Calbindin expression was normalized to β-actin expression. Densitometry was carried out with ImageJ software. Data represent mean +/− SEM (n=3, *p<0.05, significantly different from AhR$^{fx/fx}$Math1$^{+/+}$, Student's t-test). Western blots are representative of 3 independent experiments.

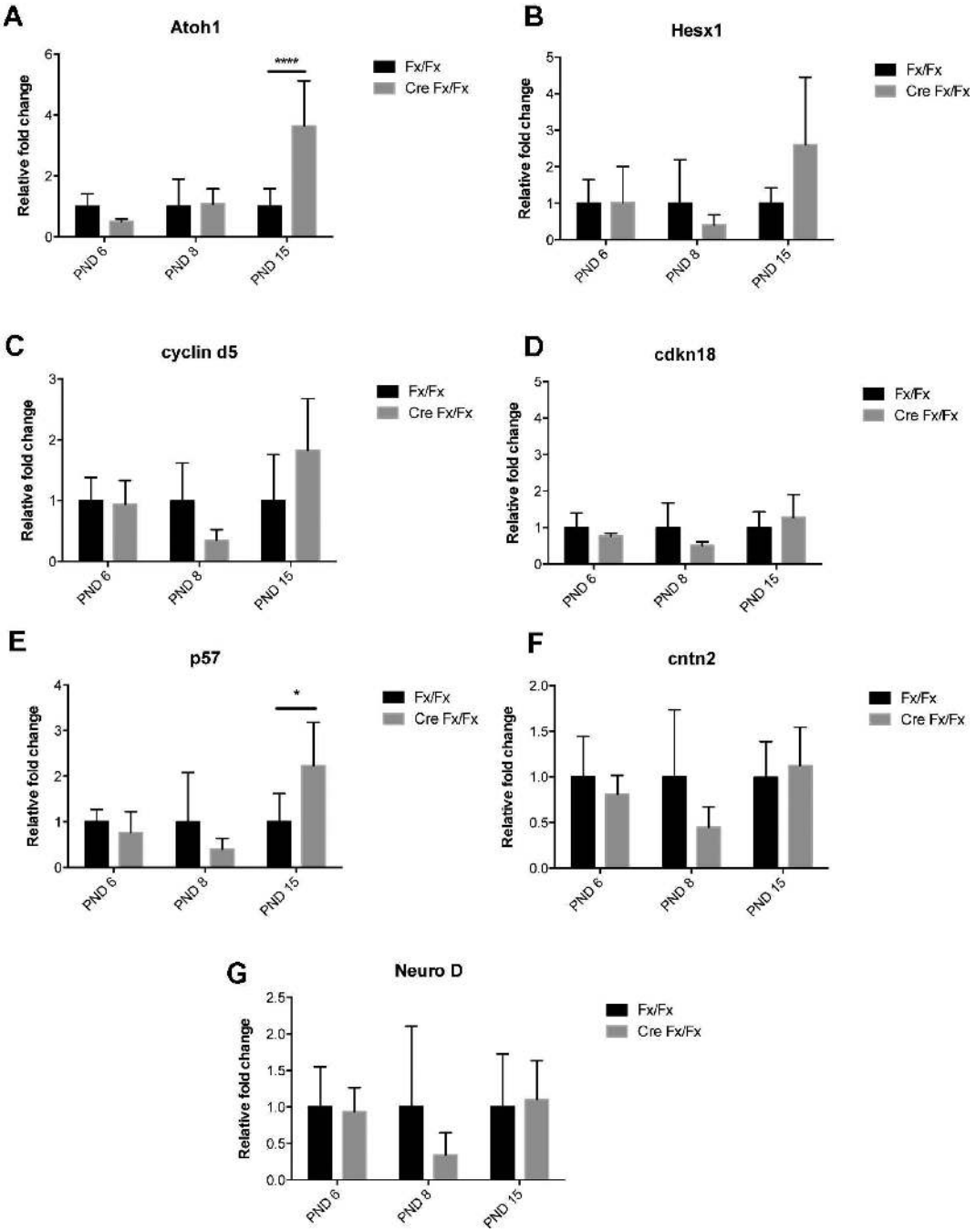

Fig 9. Granule neuron precursor cell cycle related genes are altered in AhR CKO mice throughout early postnatal development

GNPs were harvested from AhR CKO or wild type cerebella at various time points indicated and mRNA was processed for QPCR analyses of essential GNP cell cycle related transcripts. **(A-C)** Expression of key pro-proliferative GNP transcripts. (**D-E)** Expression of cell cycle checkpoint G_1/S cyclin dependent kinase inhibitors**. (F-G)** Expression of essential early differentiation and migratory GNP transcripts. All transcripts were normalized to 18S. Data

represent mean +/− SEM (n=5, *p<0.05, ***p<0.001, significantly different from $AhR^{fx/fx}Math1^{+/+}$, Student's t-test).